



Temporal and spatial distribution of $K_d(490)$ and its response to precipitation and wind in Lake Hongze based on MODIS data

Shaohua Lei^a Qiao Wang^b Yunmei Li^{a*} Heng Lv^a Ge Liu^c Zhubin Zheng^d

Chengong Du^a Meng Mu^a Jie Xu^a Shun Bi^a Song Miao^a Shuai Zeng^a

^a Jiangsu Center for Collaborative Innovation in Geographical Information Resource Development and Application, Key Laboratory of Virtual Geographical Environment of Ministry of Education, College of Geographical Science, Nanjing Normal University, Nanjing, China;
^b Satellite Environmental Center, Ministry of Environmental Protection of the People's Republic of China, Beijing, China;
^c Northeast Institute of Geography and Agricultural Ecology, Chinese Academy of Sciences, Changchun, China;
^d School of Geography and Environmental Engineering, Gannan Normal University, Ganzhou, China;



Abstract

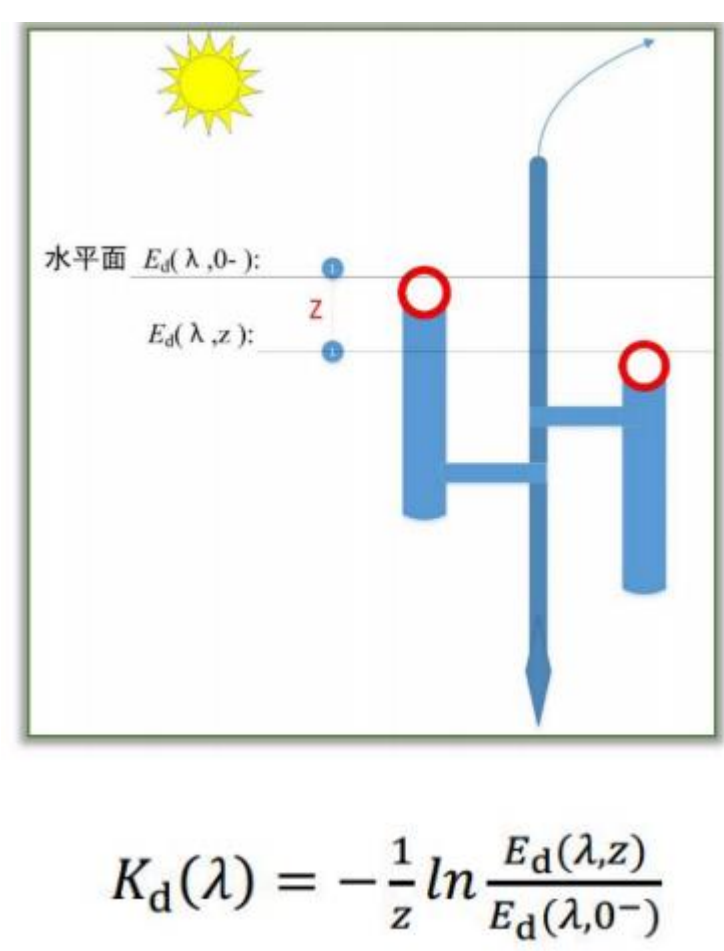
The diffuse attenuation coefficient $K_d(\lambda)$ is an important optical parameter that can be determined remotely. It plays a meaningful role in inland and coastal biogeochemical processes and aids in determining water quality. Four data-gathering expeditions were conducted in Lake Hongze (HZZ), China, between 2015 and 2017. Based on the *in situ* optical and biological data, we constructed and evaluated a regional empirical model for retrieving $K_d(490)$ of HZZ from MODIS/Aqua images between 2002 and 2016. Our results are as follows: (1) The developed algorithm, using the visible bands ($R_{rs}(\text{green})/R_{rs}(\text{red})$), performs **robustly for $K_d(490)$ estimation**, with R^2 of 0.82 and $P < 0.0001$ for the modeling data. By validating with the *in situ* observed data, the mean absolute percentage error is determined to be 17.82%, and the root means square error is 1.52 m^{-1} . (2) The **spatial distribution** of $K_d(490)$ strongly relates with the input river that formed a cone-shaped distribution with the vertex at Huai River Estuary, decreasing from the southeast (RC) to the northern (NE) and western bays (WL and CZL) in HZZ. The largest $K_d(490)$ value is in RC, with $7.10 \pm 3.03 \text{ m}^{-1}$, followed by NE and WL with values of $6.10 \pm 2.58 \text{ m}^{-1}$ and $5.32 \pm 2.09 \text{ m}^{-1}$, respectively. (3) $K_d(490)$ reaches high values in winter and low values in the summer although the variance is quite different in different lake areas. The **seasonal distribution** of $K_d(490)$ in HZZ is driven by the runoff produced by precipitation. (4) $K_d(490)$ **decreased** systematically as the East Asian monsoon weakened from 2002 to 2012 that means wind has great influence on $K_d(490)$ variation from year scale. However, human activity like sand-mining disrupted this trend, leading to the **rise** of $K_d(490)$ during 2012 and 2016.

Introduction

The health of aquatic ecosystems affects the primary productivity of water bodies, thus further influencing carbon production. Therefore, it is necessary to evaluate and monitor aquatic ecosystems in inland waters to **further global climate and environmental research**. Since the penetration and availability of light below the water surface are necessary for the existence of a water ecosystem (Mobley, 1994), the diffuse attenuation coefficient $K_d(\lambda)$ is usually considered as a **comprehensive performance measure** of water quality. $K_d(\lambda)$ measures the transfer process of light and heat in water bodies (Platt et al., 1984; Tiwari and Shanmugam, 2014) and is, related to the following parameters:

- $K_d(\lambda) \propto \text{IOPs}$
- $K_d(\lambda) \propto \text{AOPs}$
- $K_d(\lambda) \propto Z_{SD}$
- $K_d(\lambda) \propto Z_{eu}$
- $K_d(\lambda) \propto$ "Sensed" water column thickness
- $K_d(\lambda) \propto$ Hydrodynamic force

therefore, a **useful** parameter for monitoring aquatic ecosystems.



Objective

In this study, a total of 1951 images of HZZ from 2002 to 2016 were processed, and $K_d(490)$ was derived from the images. The relationship between factors such as **precipitation, wind speed, and human activities** (such as sand dredger) were analyzed to determine the effects on $K_d(490)$ change. The main objectives were (1) to **develop an algorithm to estimate $K_d(490)$ in HZZ using MODIS data**; (2) to **retrieve the spatiotemporal variation patterns of $K_d(490)$ in HZZ**; (3) to **analyze the effects of climatic factors (rainfall, and wind) on annual and/or seasonal change**.

Study Areas

Study Areas
 HZZ ($33^{\circ}06' - 33^{\circ}40'N$, $118^{\circ}10' - 118^{\circ}52'E$) is a shallow lake with an average water depth of 1.9 m. Its area is 1597 km^2 , with a volume of 3.04 billion m^3 at a water level of 12.5 m. HZZ is located in the Huai River Basin, in a warm temperate zone that is within a **semi-humid monsoon climate region**. In order to explore the spatio-temporal differences, HZZ is divided into four regions, according to the shape of the lake and hydrological characteristics: Chengzi Lake (CZL), wetland (WL) (Tang, 2007), river channel (RC) and the remaining northeast region (NE). The four partitions are shown in Figure 1.

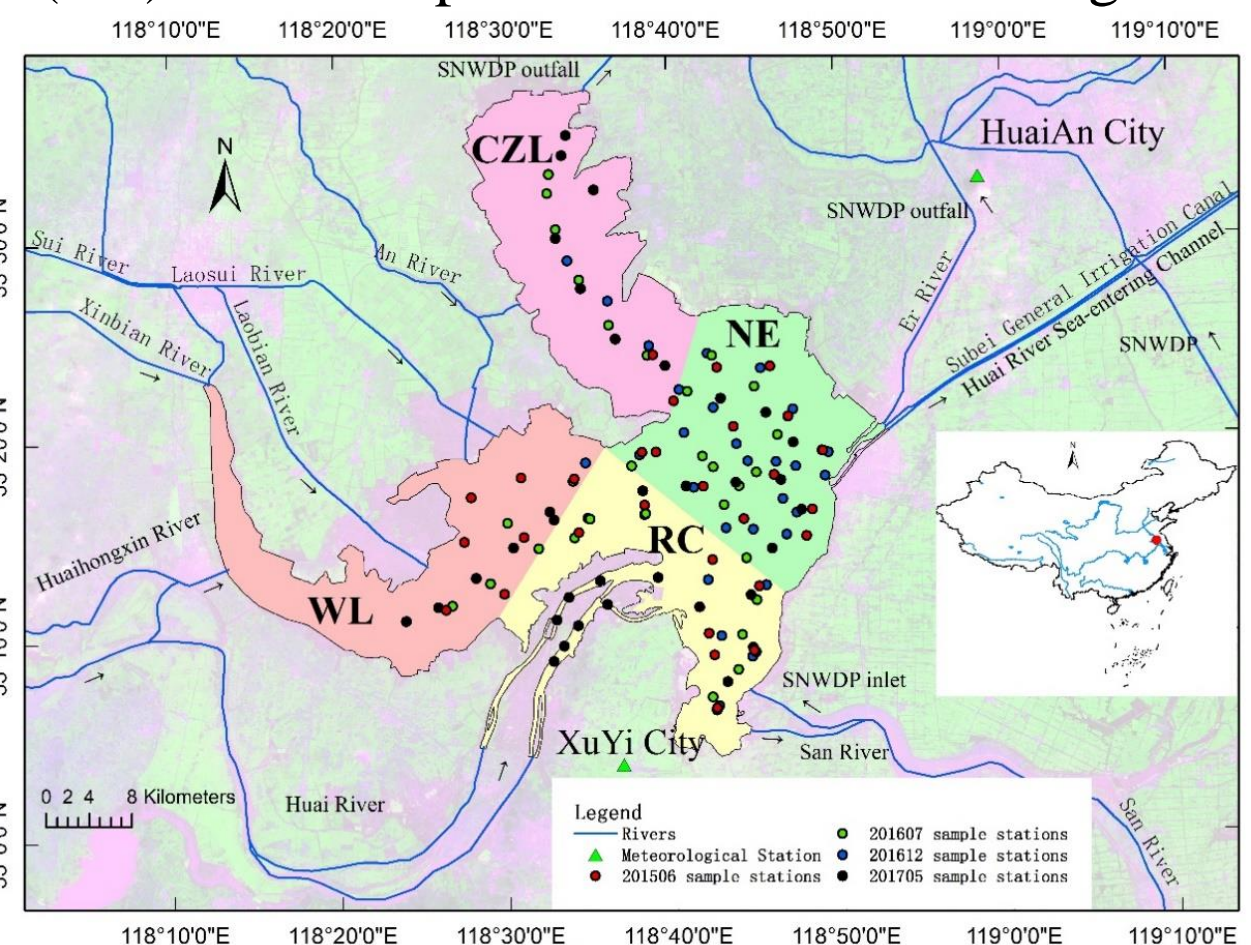


Figure 1. Location of Lake Hongze, the fourth largest freshwater lake in China. The red/green/blue/black points represent the sampling sites from four surveys in 2015-2017. The aqua blue line represents the river and the East Route of SNWDP, and the black arrows show the water flow directions.

Data and Methods

Climate data

Monthly precipitation and wind speed were measured at two meteorological stations near HZZ (HuaiAn City and XuYi City, as illustrated in Figure 1) in the Huai River Basin from the China Meteorological Data Sharing Service System (<http://cdc.cma.gov.cn/>).

MODIS/Aqua image acquisition and pre-processing

A total of **1951** MODIS/Aqua Level-0 images of HZZ between July 2002 and December 2016 were downloaded from NASA's archive (<https://oceandata.sci.gsfc.nasa.gov/>), as were the corresponding spectral response function (SRF) and calibration data. Radiometric calibration and geometric correction were completed using SeaWiFS Data Analysis System (SeaDAS). Then, an improved land target-based atmospheric correction method (Liu et al., 2016) was used to derive R_{rs} .

Model development and validation

In order to build the best fit to the data used, band ratios incorporating all possible combinations of MODIS/Aqua from visible to near-infrared bands of R_{rs} are calibrated with the linear, quadratic, cubic, power, exponential, and logarithm functions. The single band (Shi et al., 2014), ratio (Zheng et al., 2016), ratios combination algorithms were attempted to estimate $K_d(490)$ also shown in table 5. The results revealed an exponential fitting relationship between $R_{rs}(645)/R_{rs}(555)$, and the $K_d(490)$ yielded the best fit to our dataset (Figure 2(a), $R^2 \approx 0.82$, $p < 0.0001$).

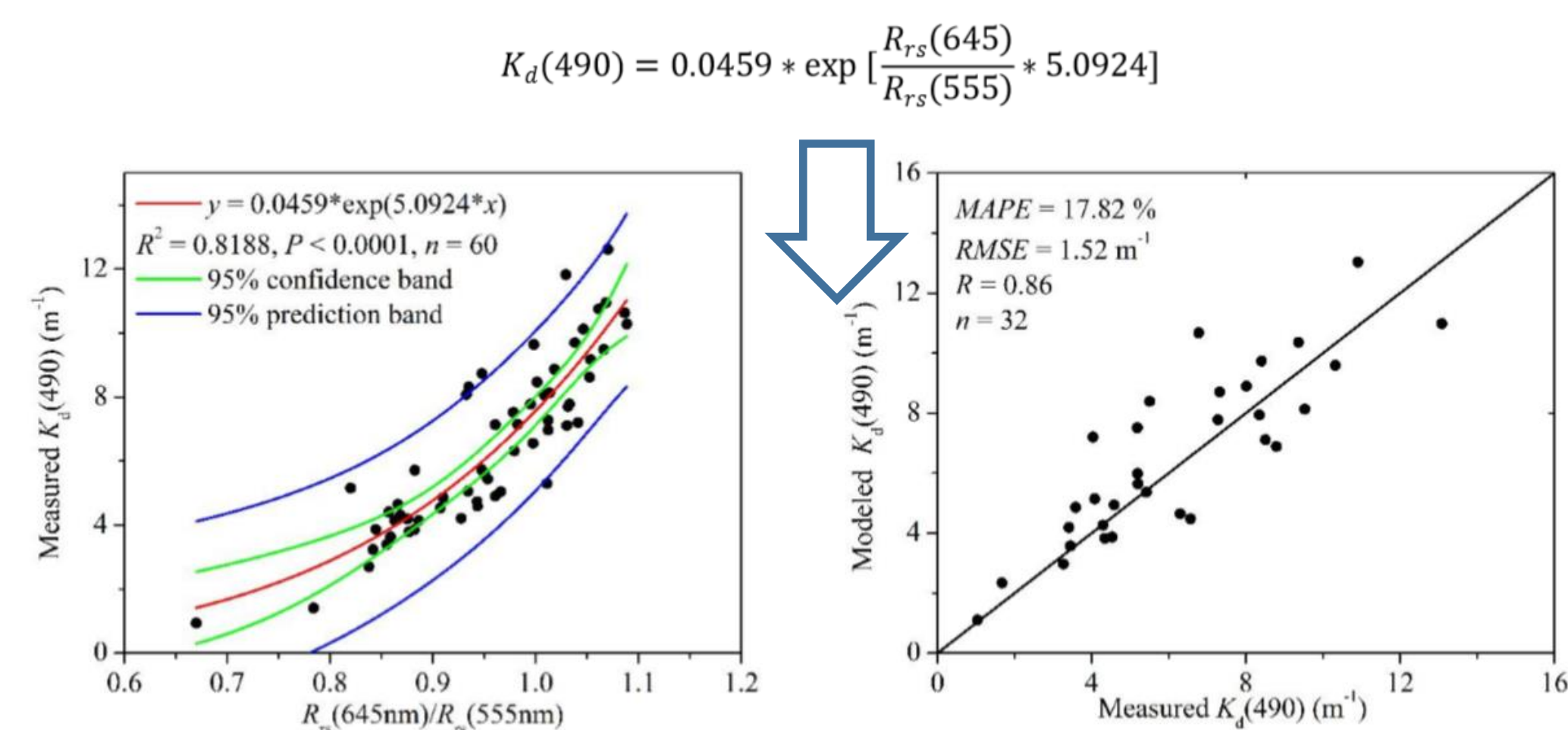


Figure 2. (a) Scatter diagram of modeling data, $n = 60$. The x-axis represents the band ratio of $R_{rs}(645)$ and $R_{rs}(555)$, and the y-axis represents $K_d(490)$. (b) Comparison between measured and estimated $K_d(490)$, $n = 32$.

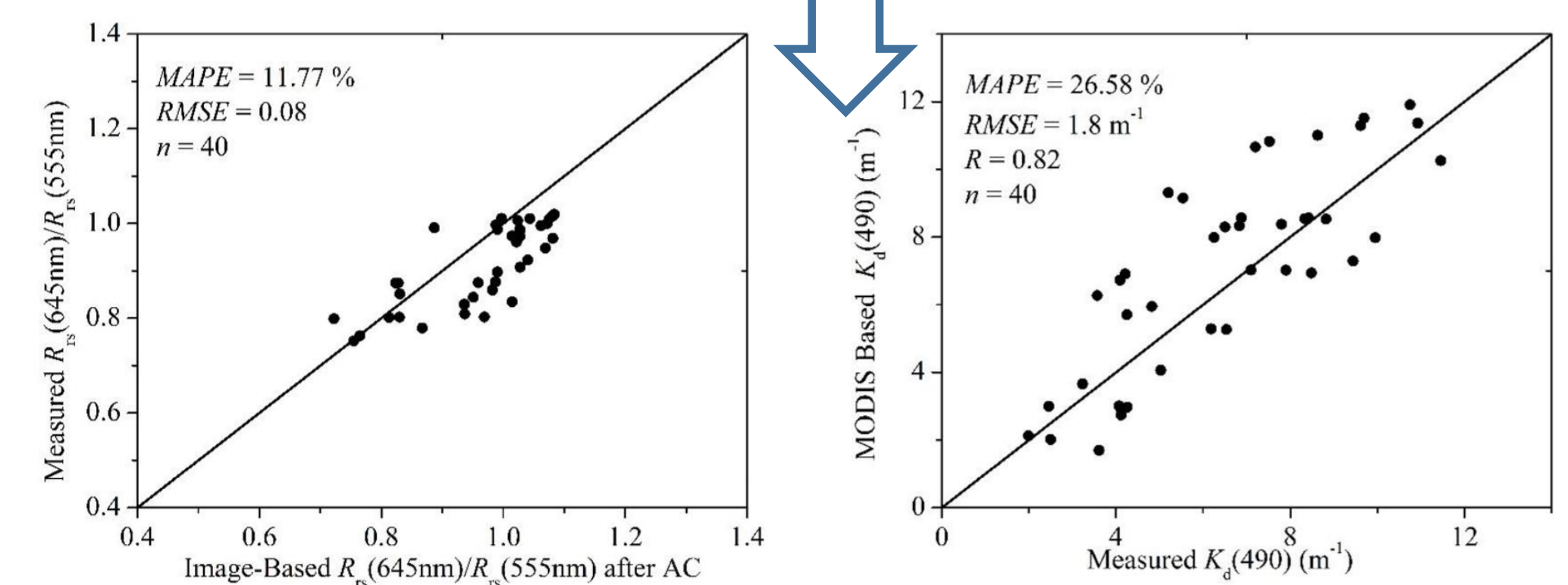


Figure 3. Atmospheric correction verification and model validation using quasi-synchronous points in the ± 3 hours of imaging time. (a) Atmospheric correction accuracy verification. (b) Comparison of measured $K_d(490)$ and MODIS/Aqua-based $K_d(490)$.

Results

The downloaded 1951 MODIS/Aqua images from 2002 to 2016 were used to generate water remote sensing reflectance using the atmospheric correction method mentioned in the previous section. These atmospherically corrected satellite image data were then used to derive spatial and temporal $K_d(490)$ distributions using the developed model. Noting that the annual and daily mean values of $K_d(490)$ do not include empty values caused by cloud cover.

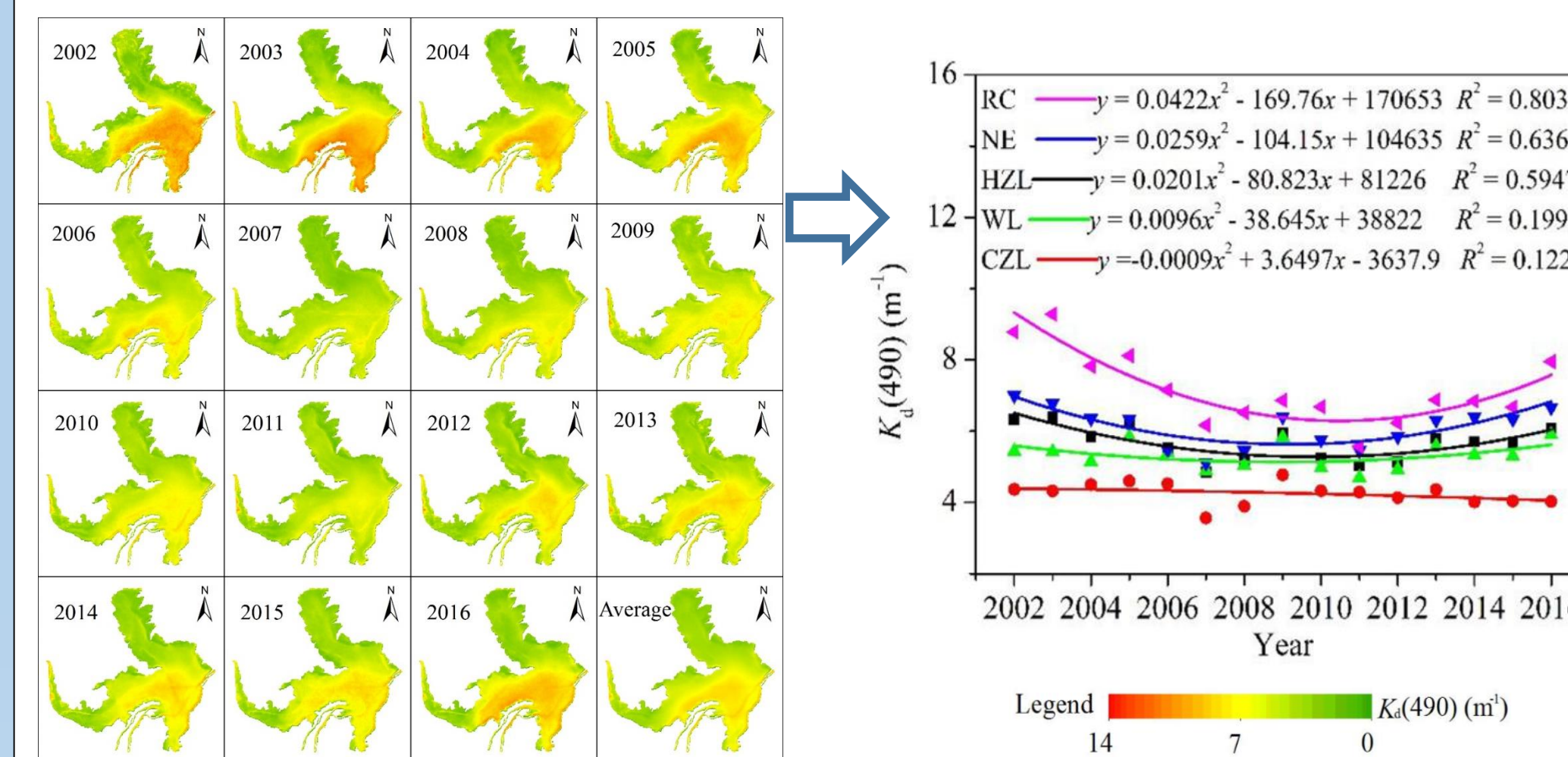


Figure 4. Annual distribution of $K_d(490)$ in HZZ from 2002 to 2016.

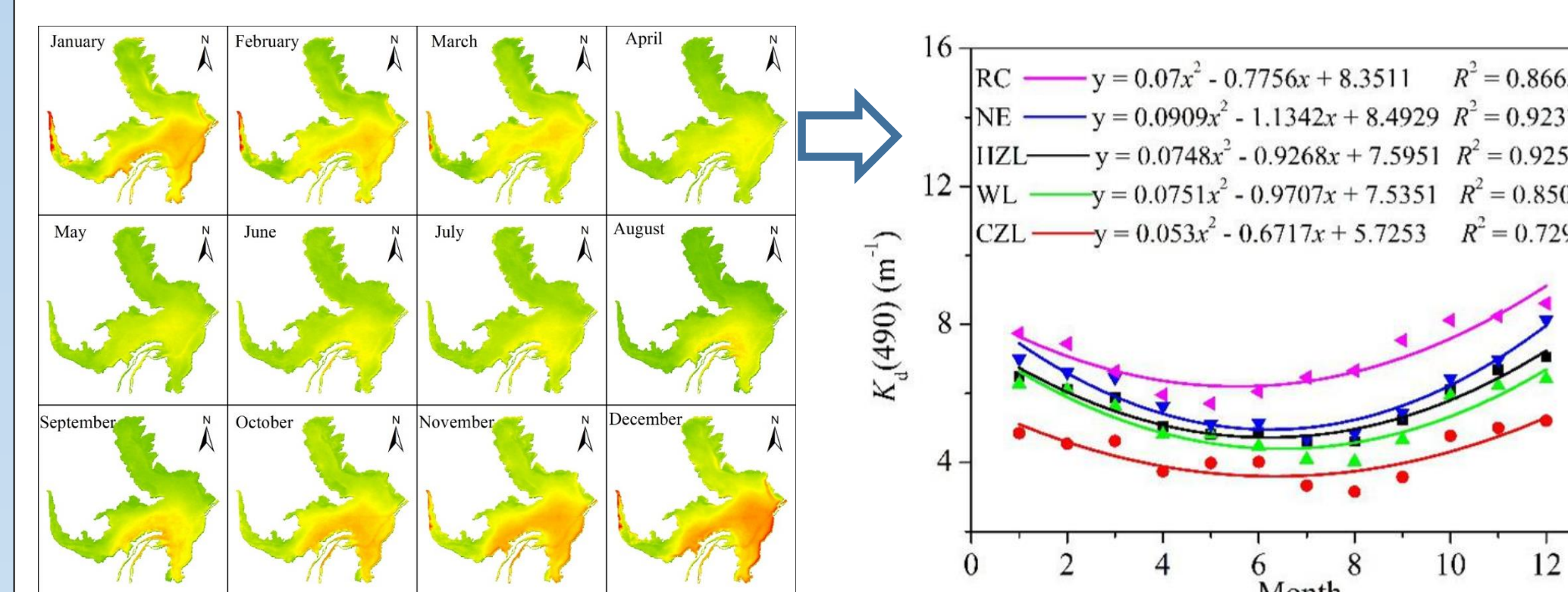


Figure 5. Monthly distribution of $K_d(490)$ in HZZ from 2002 to 2016.

Discussion

A comparison with other $K_d(490)$ estimation algorithms.

Type	Model	Equation form	R^2	MAPE(%)	RMSE(m^{-1})
single band	Shi et al.	$K_d(490) = 65.788 \cdot R_{rs}(645) + 2.4571$	0.17	35.99	2.81
band ratio	Zheng et al.	$K_d(490) = 1.7264 \cdot \ln \left(\frac{R_{rs}(645)}{R_{rs}(555)} \right) + 7.9271$	0.42	33.12	2.01
ratios	Shen et al.	$K_d(490) = 1.422 \cdot \left(\frac{R_{rs}(645)}{R_{rs}(555)} \right)^2 + 12.49 \cdot \left(\frac{R_{rs}(645)}{R_{rs}(555)} \right) - 0.754$	0.76	22.94	1.94
combination					
band ratio	Our algorithm	$K_d(490) = 0.0459 \cdot \exp \left(\frac{R_{rs}(645)}{R_{rs}(555)} \right) + 5.0924$	0.82	17.82	1.52

Our algorithm shown less difference among all the compared algorithms

The intra-annual response of $K_d(490)$ to precipitation and wind speed

To quantify the influence of precipitation and wind on $K_d(490)$ changes, a linear regression was applied to explain the annual variation between monthly precipitation data and $K_d(490)$. The most notable negative correlation appeared in the WL region (R^2 of 0.83, Figure 6), followed by NE ($R^2 = 0.75$) and CZL ($R^2 = 0.73$). A relatively poor correlation is seen in the RC area ($R^2 = 0.30$). However, a relatively higher correlation with monthly wind speed appeared in this area ($R^2 = 0.35$). That indicates that, in most part of the lake, runoff is the principal driving factor of $K_d(490)$ changes, while in the main lake entry area (RC region), both wind speed and precipitation negatively affect $K_d(490)$.

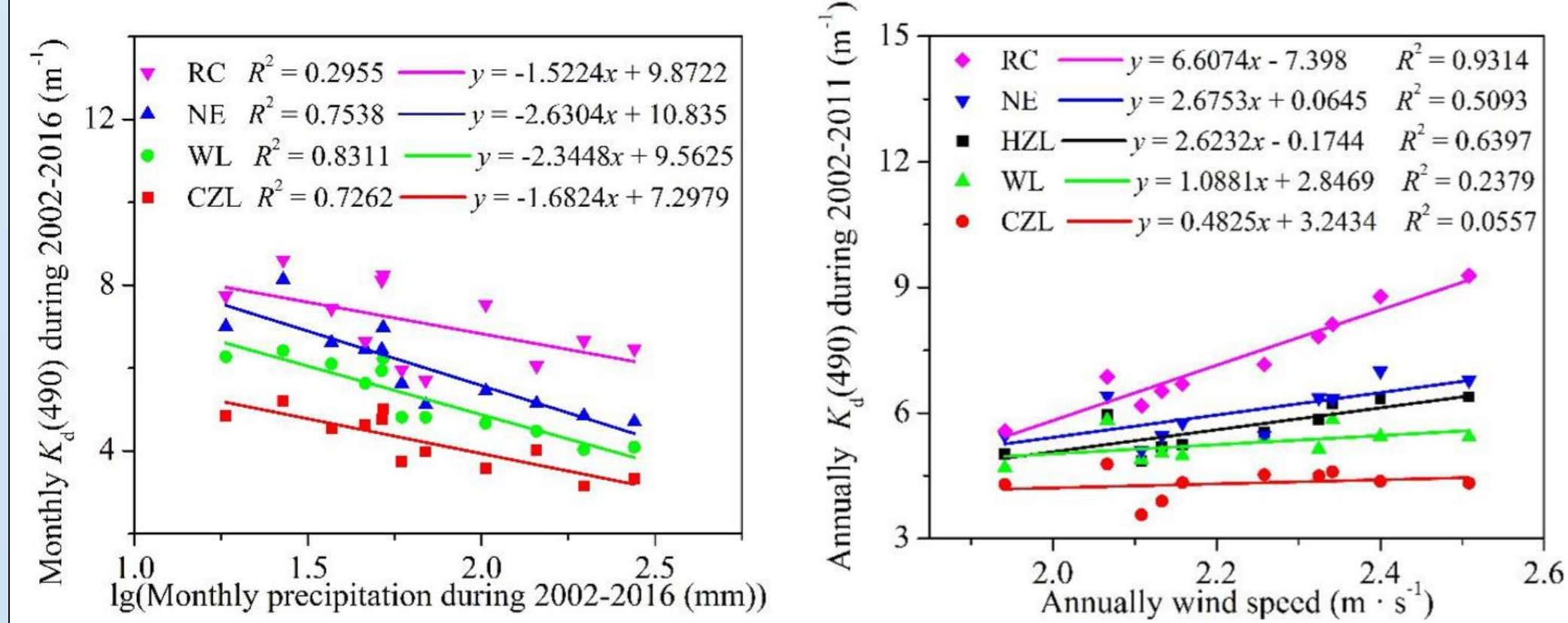


Figure 6. (Left) The relationship between monthly meteorological factors and monthly $K_d(490)$ retrieved by MODIS/Aqua from 2002 to 2016. (Right) The relationship between annual wind speed data and satellite retrieval $K_d(490)$ in HZZ and four major zones from 2002 to 2011.

The inter-annual response of $K_d(490)$ to precipitation and wind speed

What caused the fluctuation about $K_d(490)$ over the years? To answer this question, the average wind speed was calculated. Moreover, a significant downward trend in annual wind speed was found from 2002 to 2016, with a remarkable coefficient of determination of 0.88 ($P < 0.001$). Such a significant decrease in wind speed directly resulted in an inter annual decline in $K_d(490)$ in HZZ from 2002 to 2011 ($R^2 = 0.64$), especially in RC ($R^2 = 0.93$). Nevertheless, **for the first time** found in Lake Hongze of the Huai River basin, North China.

However, although the wind speed still dropped linearly after 2012, and the precipitation changed slightly compared to the previous ten years, $K_d(490)$ did not follow the previous pattern. What was the cause of the inter annual rise of $K_d(490)$ from 2012 to 2016? Rampant illegal sand mining in HZZ emerged starting in 2012 (Figure 7), which was driven by high profit. Illegal mining activities have not completely stopped, since we found a lot of dredge working in the NE. The sand mining activities have made the sediment at the lake bottom re-suspended, and that has directly increased the value of $K_d(490)$.

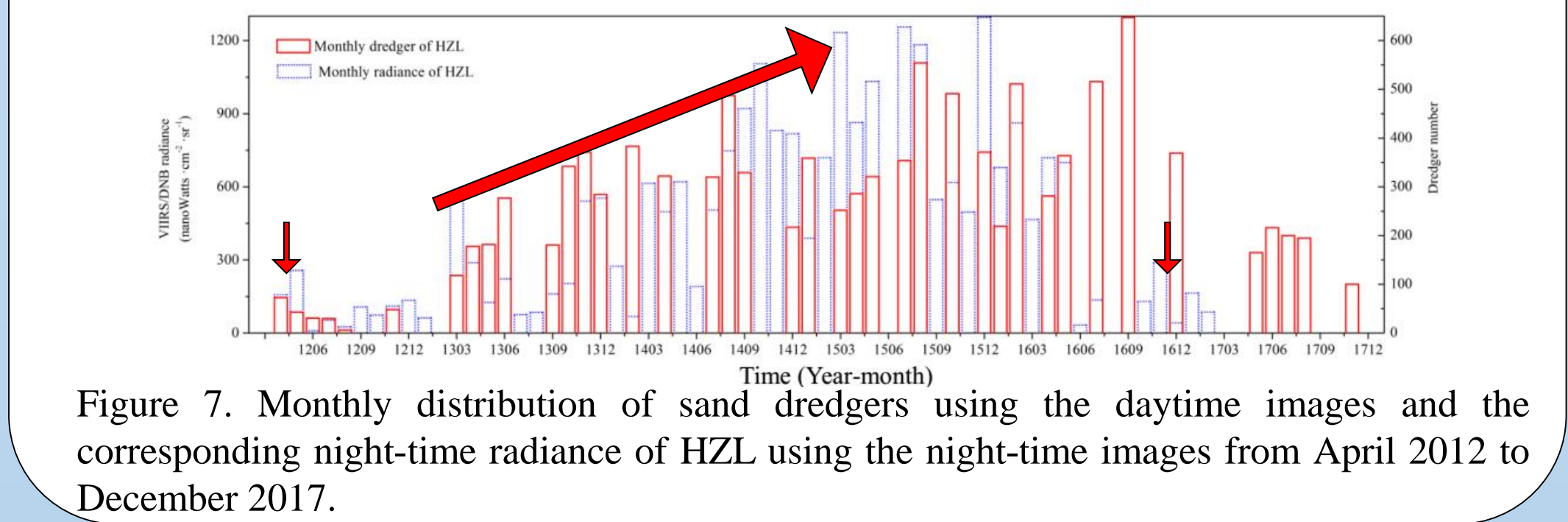


Figure 7. Monthly distribution of sand dredgers using the daytime images and the corresponding night-time radiance of HZZ using the night-time images from April 2012 to December 2017.

Conclusions

In this paper, a **robust model** was built to estimate $K_d(490)$ in Lake Hongze. Thereafter, the long-term MODIS/Aqua-derived $K_d(490)$ patterns from 2002 to 2016 were retrieved, and the **inter-annual and intra-annual** variations of $K_d(490)$ could be analyzed. Lake $K_d(490)$ variations have historically been driven by **discharge** from the Huai River and **local winds**. The most important and meaningful findings of this article are as follows:

RegionName	The intra-annual (R^2) (precipitation) (wind speed)		The inter-annual (R^2) (precipitation) (wind speed)	
	precipitation	wind speed	precipitation	wind speed
RC	34.85%	29.55%	93.14%	0.63%
NE	0.32%	75.38%	50.93%	0.74%
HZZ	0.08%	64.85%	63.97%	0.28%
WL	0.25%	83.11%	23.79%	1.47%
CZL	0.09%	72.62%	5.57%	5.68%

It is clear that $K_d(490)$ in HZZ showed a decreasing trend from 2002 to 2011, indicating that HZZ became more limpid. Reduction in wind speed in HZZ was the driving factor for the decreasing $K_d(490)$ trend in this lake and most sub-regions. Increasing sand mining activity in HZZ may be responsible for the increasing $K_d(490)$ trend between 2012 and 2016.

Our findings indicate that MODIS imagery can be suitable for quantitative monitoring of $K_d(490)$ of an extremely turbid water body, **offering important data support** in monitoring and mitigation of adverse ecosystem impacts. We hope that long-term remote sensing products can be useful to scientists who care for the ecological environment and the health of water resources.

Acknowledgment

We thank the NASA OBPG for providing all satellite data and processing software, and the China Meteorological Data Sharing Service System (<http://cdc.cma.gov.cn/>) for providing Meteorological data.